Role of PET imaging in peritoneal involvement of subcutaneous panniculitis-like T-cell lymphoma

Darren Yak Leong Chan[1,2*], Nicholas Francis Grigoropoulos[3], Amos Zhi En Tay[4], Wanying Xie[1]

1. Department of Nuclear Medicine and Molecular Imaging, Singapore General Hospital, Singapore

2. Department of Diagnostic Radiology, Tan Tock Seng Hospital, Singapore

3. Department of Haematology, Singapore General Hospital, Singapore

4. Department of Anatomical Pathology, Singapore General Hospital, Singapore

* **Correspondence:** Darren Yak Leong Chan, Tan Tock Seng Hospital, 11 Jln Tan Tock Seng, Singapore 308433, Singapore (*ylcha22mon@gmail.com*)

Radiology Case. 2022 Jun; 16(6):1-11 :: DOI: 10.3941/jrcr.v16i6.4538

ABSTRACT

Subcutaneous panniculitis-like T-cell lymphoma is a rare subtype of cutaneous T-cell lymphomas and represents less than 1% of non-Hodgkin's lymphomas. Currently, the diagnosis is based on clinical and histological findings although clinical features may be nonspecific. Often, it is localised to subcutaneous tissue without lymph node involvement. The literature is sparse but unusual presentations have been described to involve mesentery, breast and even eyelids. Fluorine-18 fluorodeoxyglucose positron-emission tomography/computed tomography has been reported to be useful in assessing disease activity, extent and treatment response in subcutaneous panniculitis-like T-cell lymphoma but we find that it can also be a diagnostic aid for atypical presentations. In our case report, we describe a patient who presented with a neck lump but did not have any other obvious cutaneous lesions. This was biopsied and had histological features in keeping with subcutaneous panniculitis-like T-cell lymphoma. Due to the atypical presentation, positron-emission tomography was crucial for detecting the extracutaneous and likely primary site of disease in the peritoneum, which hence guided the subsequent biopsy to this affected area and confirmed the diagnosis.

CASE REPORT

CASE REPORT

The patient was a 30-year-old gentleman who initially presented with a left neck lump to the otolaryngology outpatient clinic which was likely a subcutaneous nodule. This was biopsied and demonstrated fibroadipose tissue showing an infiltrate of atypical intermediate sized lymphocytes with irregular nuclei, showing prominent rimming of adipocytes. The neoplastic lymphoid cells which were diffusely immunoreactive to pan-T cell marker CD3 and were CD8-positive with expression of cytotoxic molecules granzyme-B and TiA-1, with a high proliferation index of 80%. There was also expression of T-cell beta-F1 hemireceptor, while appearing mostly negative for T-cell delta hemireceptor (for which expression was favoured to represent an accompanying innate immure response). CD30, CD4, CD56, in-situ hybridisation for EBV and B cell marker CD20 were negative (Figure 1). Overlying skin was not included for assessment in this biopsy.

The main consideration based on these findings was subcutaneous panniculitis-like T-cell lymphoma (SPTCL) although it was recommended to exclude other dermatologic findings such as epidermotropism which would be inconsistent with SPTCL.

He was subsequently referred to the oncology department but also had to be admitted on a couple of occasions due to pyrexia of unknown origin. During his inpatient stay, he also underwent extensive microbiological work up to exclude any infective causes but this was negative. A CT scan was also performed which revealed borderline splenomegaly and nonspecific peritoneal fat stranding seen in the anterior abdomen. No enlarged lymph node was identified.

The patient's antinuclear antibodies and anti-double stranded deoxyribonucleic acid tests were negative as well as his viral screen. No vegetations were identified on the transthoracic echocardiogram.

To further investigate the nonspecific fat stranding seen in the anterior abdomen as well as provide further staging, a Fluorine-18 fluorodeoxyglucose (F-18 FDG) positron-emission tomography/computed tomography (PET/CT) was later performed (Figure 2) and this demonstrated ill-defined FDG-avid subcutaneous fat-stranding posterior to the left sternocleidomastoid muscle. FDG-avid focal fat stranding was also seen in the cardiophrenic region. However, the most FDG-avid region was in the omentum and peritoneum of the anterior abdomen extending from the left hypochondrium to the left lumbar region. All these FDG-avid regions were suspicious for disease. The spleen which was borderline enlarged also demonstrated diffuse and mildly increased metabolic activity. Ascites was also detected.

On physical examination, the patient did not have any overlying skin changes or rash and the panniculitis-like appearance of the fat stranding in the anterior abdomen with FDG-avidity on PET/CT would likely represent SPTCL. A bone marrow aspirate and trephine biopsy were also carried out. This revealed that it was slightly hypocellular with erythroid and megakaryocytic hyperplasia with few haemophagocytes seen. No evidence of lymphoma was identified in the bone marrow.

For the initial treatment, he underwent 3 cycles of cyclophosphamide, hydroxydaunorubicin, Oncovin (vincristine), prednisolone and etoposide (CHOPE) with granulocyte colony-stimulating factor injections as well. However, follow-up CT scan revealed that there was progression of the fat stranding in the upper omentum of the anterior abdomen (Figure 3) and in the cardiophrenic fat. There was also interval increase in the splenomegaly and ascites. After a multidisciplinary meeting, the decision was made to switch the patient to a romidepsin, ifosfamide, carboplatin and etoposide (Ro-ICE) regime instead due to primary refractoriness to the CHOPE regime.

A subsequent open biopsy was performed on the anterior abdominal omentum when the disease also did not respond to this second regime as seen on the subsequent repeat CT (Figure 4). The biopsy results showed that the omental tissue was infiltrated by lymphoma recapitulating a lobular (panniculitis-like) adipocytotropic pattern with fat necrosis and areas of sclerosis. The lymphomatous cells were T-cells retaining their beta hemireceptor positive immunophenotype with expression of cytotoxic protein Granzyme B (Figure 5). In addition, they appeared to comprise a CD8-alpha/alpha homodimer(+) subset, while being negative for the CD8-beta hemidimer, the significance of which is currently not well studied.

Given these biopsy results, the primary team continued to manage this as SPTCL and his treatment was then switched to a Gemcitabine, Dexamethasone and Cisplatin (GDP) regime thereafter.

DISCUSSION

Etiology & Demographics:

SPTCL is a rare subclassification of skin lymphomas which typically involves the subcutaneous tissues. The infiltration of subcutaneous tissues by the neoplastic cytotoxic T-cells [1] produces a panniculitis-like pattern [1]. SPTCL was first defined as a distinct entity by the World Health Organisation (WHO) in 2001 [2]. The clinical course of SPTCL was previously understood to differ depending on the T-cell receptor (TCR) phenotype of the tumour cells. Those with the TCRαβ phenotype demonstrated an indolent course. Conversely, the TCRγδ phenotype was fatal as it was more associated with haemophagocytic syndrome [3].

The classification was later updated in the World Health Organisation-European Organisation for Research and Treatment of Cancer classification (WHO-EORTC) for primary cutaneous lymphoma which restricted SPTCL to only the TCRαβ phenotype [4].

The incidence of SPTCL is less than 1% of all non-Hodgkin's lymphomas (NHLs) [2]. SPTCL is most common in young adults with a median age of 36 years, with less than 20% of them being 20 years of age or younger. SPTCL has a female predominance with the disease being twice as common in females compared to males [5].

Clinical & Imaging Findings:

Typical presentations of the disease will follow an indolent course of recurrent relapsing but self-healing subcutaneous nodules which are often painless [5]. They can also present as deep-seated plaques, usually on the trunk and extremities and can also involve the face, neck and back [6]. New nodules can reappear at the same or at different sites. It is not uncommon to see these nodules in various phases of "healing". A minority of such patients can have lymphadenopathy or hepatosplenomegaly but clinically, there is usually no evidence of lymphoma outside the subcutis. Visceral involvement is also uncommon and distant metastasis to organs is more often seen in the aforementioned cutaneous γδ T-cell lymphomas [5,7,8]. Also, about 75% of patients with SPTCL have multifocal cutaneous involvement [4].

The patient we reported did not exhibit any cutaneous lesions and other than the initial left neck lump, did not have additional subcutaneous nodules. There was also involvement outside of the subcutis as seen primarily in the anterior abdomen peritoneum and in the cardiophrenic fat. The panniculitis-like pattern in the anterior abdomen and the intense FDG-uptake seen at this region was likely related to SPTCL involvement.

Diagnosis of SPTCL can be challenging in the early stages since the cutaneous symptoms can mimic other more common dermatological conditions such as benign panniculitis, eczema, cellulitis, systemic lupus erythematosus and various inflammatory skin conditions or infections [9]. Diagnosis is also based on the histology obtained from skin or subcutaneous tissue biopsies [10] and this was even more complicated in our patient who had no obvious viable sites to biopsy. Hence, imaging was useful in guiding to the affected extracutaneous areas for biopsy to help reach and confirm the diagnosis.

A few unusual presentations of SPTCL have been described such as eyelid swelling [11], erythema nodosum [12], diffuse thoracic subcutaneous infiltration [13] as well as breast involvement [14]. There have been reports of SPTCL initially presenting with skin lesions and later involving the abdominal wall and mesentery [15] but primary involvement of sites such as the peritoneum and cardiophrenic fat without skin lesions has not been reported in living patients.

Since a histological diagnosis had already been obtained for our patient, FDG-18 PET/CT was performed as there were no skin lesions present to physically confirm the diagnosis. FDG-18 PET/CT is the main modality for detection of both nodal and visceral involvement in Hodgkin's and non-Hodgkin's lymphoma [16,17]. In a previous case series, it found that FDG-18 PET/CT provided a more accurate estimate of disease burden in cutaneous T-cell lymphomas compared to physical examination alone [18]. In addition, PET/CT was useful to determine distribution and metabolic activity of the patterns in SPTCL [14, 19-20]. It is thus sensitive in detecting abnormal FDG uptake in the involved sites. PET/CT would aid in picking up extracutaneous disease [19-22] such as in our patient such as in lymph nodes, intra-abdominal [21] and peri-renal fat [23] as reported in a few other case studies. Bone marrow involvement in SPTCL has also been identified on PET/CT [24,25].

Treatment & Prognosis:

Furthermore, standardised uptake value (SUV) was found to be elevated in subcutaneous lesions in an analysis of 8 cases varying from 1.2 to 4.7 maximum SUV on initial PET with interval reduction post treatment [26]. PET would therefore also be valuable in assessing treatment response. This is important as there is currently no consensus on the treatment of SPTCL which is even more challenging in atypical presentations.

In essence, SPTCL can be difficult to diagnose especially in cases with an atypical presentation and no skin lesions available for repeat biopsy. We recommend performing FDG-18 PET/CT in such cases to detect extracutaneous involvement and occult lesions as well as aid in guiding the biopsy of these affected areas to confirm the diagnosis.

Typically, SPTCL has a slow disease course and excellent overall prognosis with a 5-year survival rate >80% [27]. But this may not be true in atypical cases, as can be seen in the relatively rapid disease progression of our patient. Hence, especially in such scenarios, PET/CT would help to provide information regarding disease burden with accurate staging for prognosis and future surveillance.

Differential Diagnoses:

In SPTCL, the presence of hepatosplenomegaly, skin lesions, lymphadenopathy and fever can often mimic autoimmune or rheumatological conditions. The differentials could include nodular panniculitis, systemic vasculitis, dermatomyositis, lupus erythematosus profundus [28] and the idiopathic Weber-Christian disease [14]. However, specific to our patient who presented with fever, lymphadenopathy and peritoneal fat-stranding without any skin lesions, other differential diagnoses would have to be considered given the atypical location of SPTCL in the anterior abdominal omentum. These include malignant or infective conditions such as primary peritoneal serous carcinoma, peritoneal malignant mesothelioma, peritoneal carcinomatosis (from known malignancies) and tuberculous peritonitis.

Primary peritoneal serous carcinoma

Primary peritoneal serous carcinoma is an epithelial tumour arising from the peritoneum. Histologically, it resembles malignant ovarian surface epithelial stromal tumour and thought to arise from extraovarian mesothelium with Müllerian potential [29]. This disease almost always occurs in women [30,31] with few case reports in men [32]. Patients present with abdominal distension and pain [31]. Clinically, elevated serum CA-125 levels are detected. The most common cross-sectional imaging features include ascites, peritoneal nodules/thickening and omental masses. These nodules and masses enhance with contrast on CT and magnetic resonance (MR) imaging [33]. Psammomatous calcification of these nodules is seen in 30% of these cases [34,35]. Findings of ascites, peritoneal and omental nodules in a female patient with no prior evidence of a primary visceral cancer or ovarian mass should be suggestive of this condition.

Peritoneal malignant mesothelioma

Peritoneal malignant mesothelioma is an uncommon malignancy arising from mesothelial cells or multipotent subserosal mesenchymal cells. The majority of malignant mesotheliomas tend to be seen in the pleura with only 6-10% of them originating in the peritoneum [36]. They can be classified into the diffuse and localised subtypes where the former is usually highly aggressive and the latter having better prognosis [37]. There is a well-established association between malignant mesothelioma and asbestos exposure with higher levels of exposure seen in the peritoneal as opposed to pleural malignant mesothelioma [38]. This disease is also more common in men than women with the median age of presentation at 60 years [37]. Distinct patterns seen on the CT imaging depends on the subtype and demonstrates either diffuse involvement with infiltration and sheet-like peritoneal thickening (which may later become irregular and nodular) or focal intraperitoneal masses [39-42]. Ascites and omental caking are also seen which may present as fine, nodular soft tissue studding or masses. The

omental masses enhance heterogeneously on intravenous contrast [33].

Peritoneal carcinomatosis

Peritoneal carcinomatosis occurs when primaries from the gastrointestinal tract (such as colorectal cancer), ovary, uterus, breast and lung metastasise to the peritoneal surface. Patients may initially be asymptomatic but progressive involvement of the peritoneum leads to abdominal distension and pain from bowel obstruction [43]. Ascites is a common finding and loculation of ascitic fluid may be seen [44]. The imaging findings on CT can vary from multifocal discrete nodules to infiltrative masses. Thickening, nodularity and contrast enhancement of the peritoneum also suggests this underlying malignant process [45, 46]. Infiltration of the small bowel mesentery gives a characteristic pleated or stellate pattern as the mesentery becomes stiff and loses the normal undulations with straightening of mesenteric vasculature [44, 47-48].

While MR imaging is less widely used than CT, it possesses superior contrast resolution for evaluating the peritoneal cavity. Peritoneal carcinomatosis enhances slowly on intravenous gadolinium and these are best seen 5-10 minutes after administration. Enhancement of the peritoneum to a greater degree than the liver should be considered abnormal especially if there is associated thickening or nodularity [49]. MR imaging also has better sensitivity than CT for detection of nodules less than 1 cm [50]. On FDG-18 PET/CT, these metastatic foci appear as discrete areas of increased activity but subcentimetre lesions may not demonstrate adequate uptake to be identified [46]. Thus, PET/CT may aid in the diagnosis but their precise role is still unknown [51-53].

Tuberculous peritonitis

Tuberculous peritonitis is the most common clinical presentation for abdominal tuberculosis, affecting up to one-third of such patients [54]. There are three main types: wet, fibrotic and dry [55] but only the fibrotic and dry types would be considered differentials for SPTCL in our patient. The fibrotic type is typified by large omental masses and mesenteric caking with matting of the bowel loops. On CT, this appears as mottled low-attenuation masses with nodular thickening. The dry type appears as mesenteric thickening, fibrous adhesions and caseous nodules [56]. The omentum can appear smudged, caked or thickened. Peritoneal thickening with contrast enhancement is seen instead of nodular implants with irregular thickening which would be more indicative of peritoneal carcinomatosis [57].

Sclerosing peritonitis

Sclerosing peritonitis is characterised by chronic fibrotic thickening of the peritoneum [58]. It can progress to a more severe form known as encapsulating peritoneal sclerosis where the thickened peritoneum encases the small bowel loops in an "abdominal cocoon" [59], leading to recurrent small bowel obstruction. There is a well-recognised association of this severe form with continuous ambulatory peritoneal dialysis [58, 60] and chronic irritation has therefore been suggested to be the cause although the exact aetiology is unclear [61]. Other associations include tuberculosis [62] and sarcoidosis [63] but there is also an idiopathic form described in both genders and children as well [59, 64-65].

Smooth thickening and enhancement of the peritoneum is the most commonly described appearance on CT [58]. Peritoneal calcification may also be identified on CT [66] but severe encapsulation may also occur in the absence of peritoneal calcification [58]. The diffuse inflammatory process also involves the small bowel along the antimesenteric wall, causing mural fibrosis and thickening [67]. This leads to adhesions, further narrowing the bowel lumen and eventually, small bowel obstruction [58]. Contrast-enhanced CT would be the best modality for such small bowel changes and their relationship to the encapsulating peritoneum [58, 68]. In our patient, this should be considered as a differential in the initial stages as there were no other cutaneous symptoms present and the primary disease was in the peritoneum as well. Nevertheless, from the subsequent scans, no evidence of peritoneal calcification or encapsulation of small bowel was seen in our patient, who also did not display any obstructive symptoms.

TEACHING POINT

Subcutaneous panniculitis-like T-cell lymphoma (SPTCL) is a rare disease with nonspecific signs and symptoms but while the diagnosis can be achieved through physical examination and histological methods, it can still be missed and confused with other mimicking autoimmune conditions especially in atypical presentations. Extracutaneous involvement of SPTCL should not be overlooked and use of FDG-18 PET/CT may therefore be crucial for guiding biopsy to obtain the initial diagnosis as well as for follow-up and monitoring of SPTCL as FDG-18 PET/CT can also assess for disease response and/or recurrence.

REFERENCES

1. Gonzalez CL, Medeiros LJ, Braziel RM, Jaffe ES. T-cell lymphoma involving subcutaneous tissue: a clinicopathologic entity commonly associated with hemophagocytic syndrome. Am J Surg Pathol. 1991;15(1):17-27. PMID: 1985499

2. Jaffe ES, Harris NL, Stein H, Vardiman JW. Pathology and Genetics of Tumours of Haematopoietic and Lymphoid Tissues. World Health Organization Classification of Tumours. Lyon, France: IARC Press, 2001; pp. 351-2. ISBN: 9283224116

3. Takeshita M, Okamura S, Oshiro Y, et.al. Clinicopathologic differences between 22 cases of CD56-negative and CD56-positive subcutaneous panniculitis-like lymphoma in Japan. Hum Pathol. 2004 Feb;35(2):231-9. PMID: 14991542

4. Willemze R, Jaffe ES, Burg G, et.al. WHO-EORTC classification for cutaneous lymphomas. Blood. 2005;105(10):3768-85. PMID: 15692063

5. Willemze R, Jansen PM, Cerroni L, et.al. Subcutaneous panniculitis-like T-cell lymphoma: definition, classification, and prognostic factors: an EORTC Cutaneous Lymphoma Group Study of 83 cases. Blood. 2008;111(2):838-45. PMID: 17934071

6. Cassis TB, Fearneyhough PK, Callen JP. Subcutaneous panniculitis-like T-cell lymphoma with vacuolar interface dermatitis resembling lupus erythematosus panniculitis. J Am Acad Dermatol. 2004 Mar;50(3):465-9. PMID: 14988694

7. Ma L, Bandarchi B, Glusac EJ. Fatal subcutaneous panniculitis-like T-cell lymphoma with interface change and dermal mucin, a dead ringer for lupus erythematosus. J Cutan Pathol. 2005 May;32(5):360-5. PMID: 15811122

8. Guizzardi M, Hendrickx IA, Mancini LL, Monti M. Cytotoxic gamma/delta subcutaneous panniculitis-like T-cell lymphoma: report of a case with pulmonary involvement unresponsive to therapy. J Eur Acad Dermatol Venereol. 2003 Mar;17(2):219-22. PMID: 12705758

9. Sugeeth MT, Narayanan G, Jayasudha AV, Nair RA. Subcutaneous panniculitis-like T-cell lymphoma. Proc (Bayl Univ Med Cent). 2017;30(1):76-77. PMID: 28127142

10. Parveen Z, Thompson K. Subcutaneous panniculitis-like T-cell lymphoma: redefinition of diagnostic criteria in the recent World Health Organization-European Organization for Research and Treatment of Cancer classification for cutaneous lymphomas. Arch Pathol Lab Med. 2009;133(2):303-8. PMID: 19195975

11. Hashimoto, R., Uchiyama, M. & Maeno, T. Case report of subcutaneous panniculitis-like T-cell lymphoma complicated by eyelid swelling. BMC Ophthalmol. 2016;16(1),117. PMID: 27440138

12. Sun D, Zheng S, Hong YX, Chen HD, Gao XH. Subcutaneous panniculitis-like T cell lymphoma presented as erythema nodosum: A case report. Dermatol Ther. 2021 Jan;34(1):e14572. PMID: 33219732

13. Ballanger F, Barbarot S, Le Gouill S, et.al. Thoracic subcutaneous infiltration: an unusual presentation of subcutaneous panniculitis-like T-cell lymphoma. Acta Derm Venereol. 2009;89(4):427-9. PMID: 19688166

14. Schramm N, Pfluger T, Reiser MF, Berger F. Subcutaneous panniculitis-like T-cell lymphoma with breast involvement: functional and morphological imaging findings. Br J Radiol. 2010;83(989):e90-e94. PMID: 20418462

15. Wang W, Pardee TS & Beaty MW. Subcutaneous panniculitis-like T cell lymphoma with mesenteric involvement. J Hematopathol. 2012;6(3), 155-159. Available at: https://doi.org/10.1007/s12308-012-0167-3. Accessed Mar 10, 2022.

16. Tsai EY, Taur A, Espinosa L, et. al. Staging accuracy in mycosis fungoides and sezary syndrome using integrated positron emission tomography and computed tomography. Arch Dermatol. 2006;142(5):577-84. PMID: 16702495

17. Buchmann I, Reinhardt M, Elsner K, et. al. 2-(Fluorine-18)fluoro-2-deoxy-d-glucose positron emission tomography in the detection and staging of malignant lymphoma. A bicenter trial. Cancer. 2001;91(5):889-99. PMID: 11251940

18. Kuo PH, McClennan BL, Carlson K, et. al. FDG-PET/CT in the evaluation of cutaneous T-cell lymphoma. Mol Imaging Biol. 2008;10(2):74-81. PMID: 18196347

19. Babb A, Zerizer I, Naresh KN, Macdonald D. Subcutaneous panniculitis-like T-cell lymphoma with extracutaneous dissemination demonstrated on FDG PET/CT. Am J Hematol 2011;86(4):375-6. PMID: 21442643

20. Rodriguez VR, Joshi A, Peng F, Rabah RM, Stockmann PT, Sava?an S. Positron emission tomography in subcutaneous panniculitis-like T-cell lymphoma. Pediatr Blood Cancer 2009;52(3):406-8. PMID: 18985722

21. Mitsuhashi K, Momose M, Masuda A, Tsunemi Y, Motoji T. Positron emission tomography revealed diffuse involvement of the lower legs and occult extracutaneous lesions in subcutaneous panniculitis-like T-cell lymphoma. Clin Nucl Med 2013;38(3):209-11. PMID: 23354029

22. Wang SY, Wu YW, Hsiao CH, Li MF, Hsu PY, Yen RF. F-18 FDG PET images for subcutaneous panniculitis like T-cell lymphoma. Clin Nucl Med 2011;36(1):66-9. PMID: 21157218

23. Ravizzini G, Meirelles GS, Horwitz SM, Grewal RK. F-18 FDG uptake in subcutaneous panniculitis-like T-cell lymphoma. Clin Nucl Med. 2008;33(12):903-5. PMID: 19033805

24. Huang CT, Yang WC, Lin SF. Positron-emission tomography findings indicating the involvement of the whole body skin in subcutaneous panniculitis-like T cell lymphoma. Ann Hematol. 2011;90(7):853-54. PMID: 20972680

25. Brown NA, Ross CW, Gudjonsson JE, et al. Subcutaneous panniculitis-like T-cell lymphoma with bone marrow involvement. Am J Clin Pathol. 2015;143(2):265-73. PMID: 25596253

26. Kim JW, Chae EJ, Park YS, et al. Radiological and clinical features of subcutaneous panniculitis-like T-cell lymphoma. J Comput Assist Tomogr. 2011;35(3):394-401. PMID: 21586937

27. Alsomali DY, Bakshi N, Kharfan-Dabaja M, Fakih RE, Aljurf M. Diagnosis and treatment of subcutaneous panniculitis-like T-cell lymphoma: A systematic literature review. Hematol Oncol Stem Cell Ther. 2021:S1658-3876(21)00051-0. Available at: https://doi.org/10.1016/j.hemonc.2021.04.001. Epub ahead of print. PMID: 34015273.

28. Yi L, Qun S, Wenjie Z, et al. The presenting manifestations of subcutaneous panniculitis-like T-cell lymphoma and T-cell lymphoma and cutaneous gammadelta T-cell lymphoma may mimic those of rheumatic diseases: A report of 11 cases. Clin Rheumatol. 2013;32(8):1169-75. PMID: 23588884

29. Muto MG, Welch WR, Mok SC, et al. Evidence for a multifocal origin of papillary serous carcinoma of the peritoneum. Cancer Res. 1995;55(3):490-492. PMID: 7834614

30. Schorge JO, Muto MG, Lee SJ, et al. BRCA1-related papillary serous carcinoma of the peritoneum has a unique molecular pathogenesis. Cancer Res. 2000;60(5):1361-1364. PMID: 10728699

31. Truong LD, Maccato ML, Awalt H, Cagle PT, Schwartz MR, Kaplan AL. Serous surface carcinoma of the peritoneum: a clinicopathologic study of 22 cases. Hum Pathol. 1990;21(1):99-110. PMID: 1688545

32. Shmueli E, Leider-Trejo L, Schwartz I, Aderka D, Inbar M. Primary papillary serous carcinoma of the peritoneum in a man. Ann Oncol. 2001;12(4):563-567. PMID: 11398893

33. Levy AD, Arnáiz J, Shaw JC, Sobin LH. Primary peritoneal tumors: Imaging features with pathologic correlation. RadioGraphics. 2008;28(2):583-607. PMID: 18349460

34. Chiou SY, Sheu MH, Wang JH, Chang CY. Peritoneal serous papillary carcinoma: a reappraisal of CT imaging features and literature review. Abdom Imaging. 2003;28(6):815-819. PMID: 14753596

35. Stafford-Johnson DB, Bree RL, Francis IR, Korobkin M. CT appearance of primary papillary serous carcinoma of the peritoneum. AJR Am J Roentgenol. 1998;171(3):687-689. PMID: 9725296

36. Attanoos RL, Gibbs AR. Pathology of malignant mesothelioma. Histopathology. 1997;30(5):403-418. PMID: 9181361

37. Churg A, Cagle PT, Roggli VL. Tumors of the serosal membranes. Silver Spring, Md: ARP, 2006. ISBN: 1881041972

38. Roggli VL, Sharma A, Butnor KJ, Sporn T, Vollmer RT. Malignant mesothelioma and occupational exposure to asbestos: a clinicopathological correlation of 1445 cases. Ultrastruct Pathol. 2002;26(2):55-65. PMID: 12036093

39. Guest PJ, Reznek RH, Selleslag D, Geraghty R, Slevin M. Peritoneal mesothelioma: the role of computed tomography in diagnosis and follow up. Clin Radiol. 1992;45 (2):79-84. PMID: 1737433

40. Puvaneswary M, Chen S, Proietto T. Peritoneal mesothelioma: CT and MRI findings. Australas Radiol. 2002;46(1):91-96. PMID: 11966596

41. Ros PR, Yuschok TJ, Buck JL, Shekitka KM, Kaude JV. Peritoneal mesothelioma: radiologic appearances correlated with histology. Acta Radiol. 1991;32(5):355-358. PMID: 1910986

42. Whitley NO, Brenner DE, Antman KH, Grant D, Aisner J. CT of peritoneal mesothelioma: analysis of eight cases. Am J Roentgenol. 1982;138(3):531-535. PMID: 6978005

43. Sadeghi B, Arvieux C, Glehen O, et al. Peritoneal carcinomatosis from non-gynecologic malignancies: results of the EVOCAPE 1 multicentric prospective study. Cancer. 2000;88(2):358-363. PMID: 10640968

44. Walkey MM, Friedman AC, Sohotra P, Radecki PD. CT manifestations of peritoneal carcinomatosis. Am J Roentgenol. 1988;150(5):1035-1041. PMID: 3258703

45. Jacquet P, Jelinek JS, Steves MA, Sugarbaker PH. Evaluation of computed tomography in patients with peritoneal carcinomatosis. Cancer. 1993;72(5):1631-1636. PMID: 8348494

46. Levy AD, Shaw JC, Sobin LH. Secondary tumors and tumorlike lesions of the peritoneal cavity: Imaging features with pathologic correlation. RadioGraphics. 2009;29(2):347-373. PMID: 19325052

47. Hamrick-Turner JE, Chiechi MV, Abbitt PL, Ros PR. Neoplastic and inflammatory processes of the peritoneum, omentum, and mesentery: diagnosis with CT. RadioGraphics. 1992;12(6):1051-1068. PMID: 1439011

48. Whitley NO, Bohlman ME, Baker LP. CT patterns of mesenteric disease. J Comput Assist Tomogr. 1982;6(3):490-496. PMID: 7096694

49. Low RN. MR imaging of the peritoneal spread of malignancy. Abdom Imaging. 2007;32(3):267-283. PMID: 17334873

50. Low RN, Barone RM, Lacey C, Sigeti JS, Alzate GD, Sebrechts CP. Peritoneal tumor: MR imaging with dilute oral barium and intravenous gadolinium containing contrast agents compared with unenhanced MR imaging and CT. Radiology. 1997;204(2): 513-520. PMID: 9240546

51. Pannu HK, Bristow RE, Cohade C, Fishman EK, Wahl RL. PET-CT in recurrent ovarian cancer: initial observations. RadioGraphics. 2004;24(1):209-223. PMID: 14730047

52. Tanaka T, Kawai Y, Kanai M, Taki Y, Nakamoto Y, Takabayashi A. Usefulness of FDG-positron emission tomography in diagnosing peritoneal recurrence of colorectal cancer. Am J Surg. 2002;184(5):433-436. PMID: 12433608

53. Turlakow A, Yeung HW, Salmon AS, Macapinlac HA, Larson SM. Peritoneal carcinomatosis: role of (18)F-FDG PET. J Nucl Med. 2003;44(9):1407-1412. PMID: 12960184

54. Zissin R, Gayer G, Kots E, Werner M, Shapiro-Feinberg M, Hertz M. Iliopsoas abscess: a report of 24 patients diagnosed by CT. Abdom Imaging. 2001;26(5):533-539. PMID: 11503095

55. Leder RA, Low VH. Tuberculosis of the abdomen. Radiol Clin North Am. 1995;33(4):691-705. PMID: 7610239

56. Burrill J, Williams CJ, Bain G, Conder G, Hine AL, Misra RR. Tuberculosis: A radiologic review. RadioGraphics. 2007;27(5):1255-1273. PMID: 17848689

57. Suri S, Gupta S, Suri R. Computed tomography in abdominal tuberculosis. Br J Radiol. 1999;72(853):92-98. PMID: 10341698

58. Ti JP, Al-Aradi A, Conlon PJ, Lee MJ, Morrin MM. Imaging features of encapsulating peritoneal sclerosis in

continuous ambulatory peritoneal dialysis patients. Am J Roentgenol. 2010;195(1):W50-W54. PMID: 20566781

59. Foo KT, Ng KC, Rauff A, Foong WC, Sinniah R. Unusual small intestinal obstruction in adolescent girls: the abdominal cocoon. Br J Surg. 1978;65(6): 427-430. PMID: 656764

60. Rigby RJ, Hawley CM. Sclerosing peritonitis: the experience in Australia. Nephrol Dial Transplant. 1998;13(1):154-159. PMID: 9481732

61. Lee RG. Sclerosing peritonitis. Dig Dis Sci. 1989;34(9):1473-1476. PMID: 2766916

62. Kaushik R, Punia RPS, Mohan H, Attri AK. Tuberculous abdominal cocoon: a report of 6 cases and review of the literature. World J Emerg Surg. 2006;1:18. PMID: 16800898

63. Ngô Y, Messing B, Marteau P, et al. Peritoneal sarcoidosis: an unrecognized cause of sclerosing peritonitis. Dig Dis Sci. 1992;37(11):1776-1780. PMID: 1425080

64. Demir MK, Akinci O, Onur E, Koksal N. Case 108: sclerosing encapsulating peritonitis. Radiology. 2007;242(3):937-939. PMID: 17325076

65. Sahoo SP, Gangopadhyay AN, Gupta DK, Gopal SC, Sharma SP, Dash RN. Abdominal cocoon in children: a report of four cases. J Pediatr Surg. 1996; 31(7):987-988. PMID: 8811577

66. Kawaguchi Y, Kawanishi H, Mujais S, Topley N, Oreopoulos DG. Encapsulating peritoneal sclerosis: definition, etiology, diagnosis, and treatment. International Society for Peritoneal Dialysis Ad Hoc Committee on Ultrafiltration Management in Peritoneal Dialysis. Perit Dial Int. 2000;20(suppl 4):S43-S55. PMID: 11098928

67. George C, Al-Zwae K, Nair S, Cast JEI. Computed tomography appearances of sclerosing encapsulating peritonitis. Clin Radiol. 2007;62(8):732-737. PMID: 17604760

68. Loughrey GJ, Hawnaur JM, Sambrook P. Case report: computed tomographic appearance of sclerosing peritonitis with gross peritoneal calcification. Clin Radiol. 1997;52(7):557-558. PMID: 9240712

FIGURES

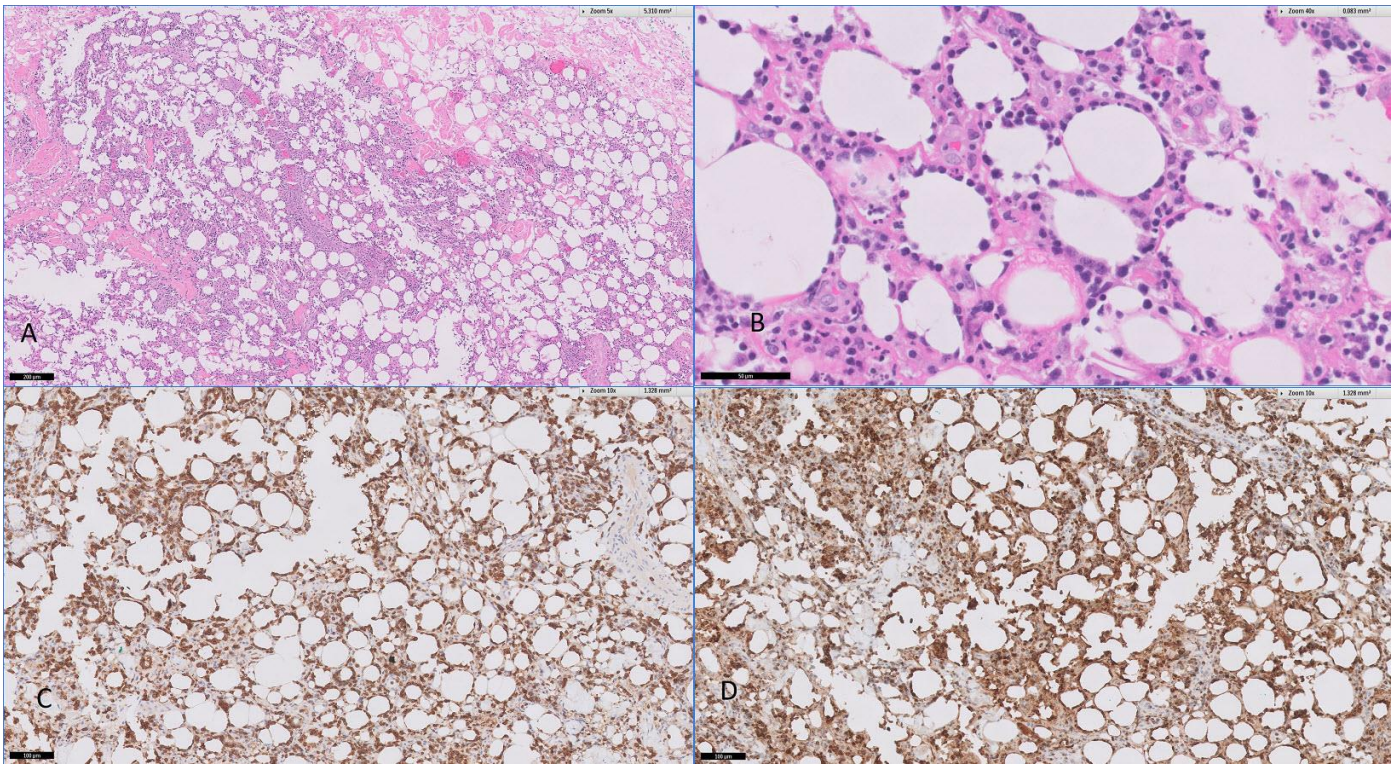

Figure 1: A 30-year-old gentleman with SPTCL presenting initially with a subcutaneous nodule at the left neck. Histology of this nodule is as described below:
Findings: Hematoxylin and eosin (H&E) stain (magnification 5x) demonstrates fibroadipose tissue which shows a panniculitis-like lymphocytic infiltrate (Figure 1A). On higher magnification (40x), intermediate-sized atypical lymphocytes with irregular nuclei are seen to rim adipocytes (Figure 1B). The lymphoproliferation comprises a CD3-positive T-cell population (Figure 1C). The T-lymphoproliferation shows a cytotoxic phenotype, with diffuse expression of Granzyme B (Figure 1D). Overall, these findings are compatible with SPTCL.

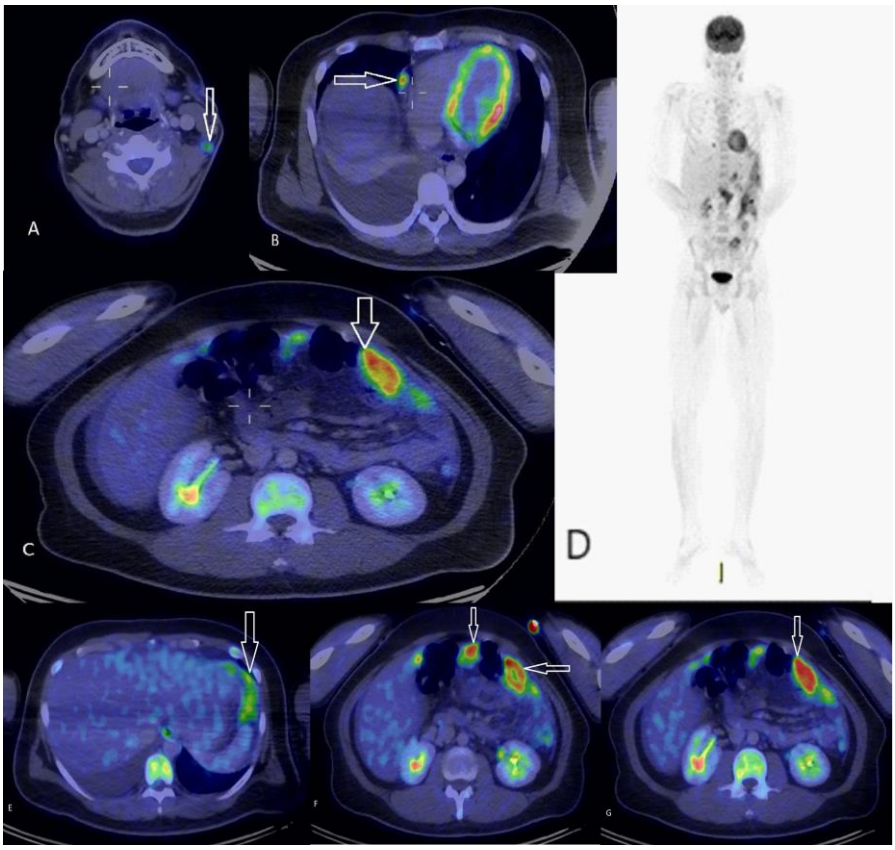

Figure 2: A 30-year-old gentleman with SPTCL involving various sites with the primary disease in the anterior abdominal omentum. Whole-body positron emission tomography/computed tomography.

FINDINGS: A whole-body positron emission tomography/computed tomography (PET/CT) reveals an ill-defined FDG avid subcutaneous fat-stranding which is seen posterior to the left sternocleidomastoid muscle (SUVmax 5.2, Figure 2A, white arrow). This represents disease involvement and likely the site of prior biopsy. FDG avid focal fat stranding is also noted at the cardiophrenic region (SUVmax 8.9, Figure 2B, white arrow). FDG avid areas of fat stranding in the omentum in the anterior abdomen (SUVmax 11.9, Figure 2C, white arrow). Whole body PET MIP image provides an overview of these abovementioned sites of disease involvement (Figure 2D). The FDG avid areas of fat stranding in the anterior abdominal omentum/peritoneum extends from the left hyponchrondrium to the left lumbar region (Figures 2E, 2F and 2G, white arrows).
TECHNIQUE: PET/CT imaging was performed from the vertex of the skull to the feet at 75 minutes after IV administration of 13.0 mCi of F-18 Fluorodeoxyglucose (FDG). Enhanced CT was performed for the purpose of attenuation correction and anatomical localization. 130ml of Omnipaque 350 was administered. Slice thickness: 3.75 mm.

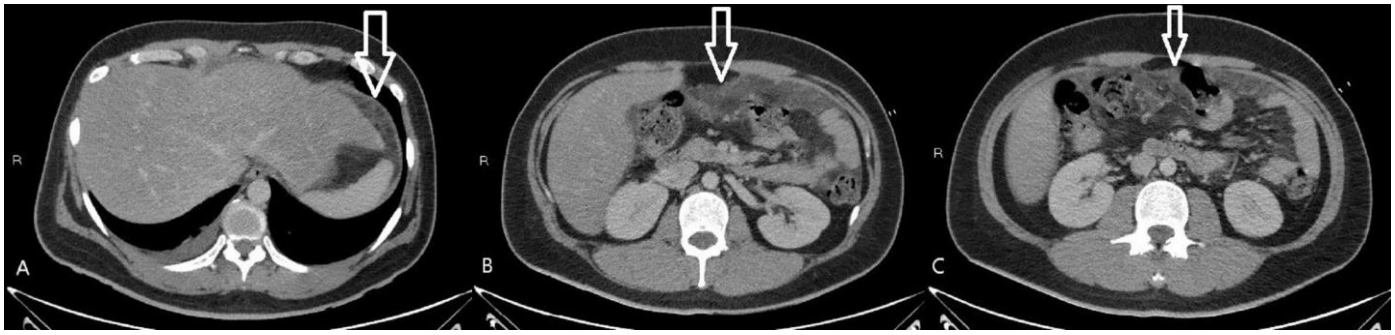

Figure 3: A 30-year-old gentleman with SPTCL, on a follow-up scan post initial, first round of chemotherapy regime. Contrast-enhanced computed tomography of the abdomen/pelvis.

FINDINGS: Interval increase of the large area of fat stranding of the anterior omentum bilaterally (Figure 3C, white arrow) and slightly more on the left (Figure 3B, white arrow) with increasing soft tissue density interspersed with fat, when compared to Figures 2F and 2G, representing disease progression. Area of focal fat stranding also again seen in the left hypochondrium (Figure 3A).
TECHNIQUE: A total of 80ml of Ultravist 370 was administered. Contrast-enhanced axial images in the soft tissue window, on portal venous phase.

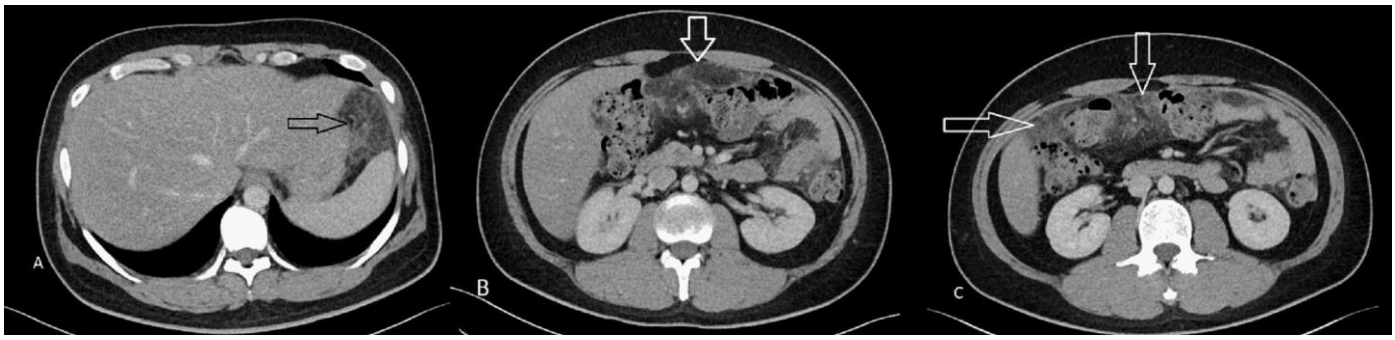

Figure 4: A 30-year-old-gentleman with SPTCL having refractory disease on the follow-up scan despite changing to a new, second round of chemotherapy regime. Contrast-enhanced computed tomography of the abdomen/pelvis.

FINDINGS: The focal nodular fat-stranding in the upper left hypochondrium is more prominent and extensive (Figure 4A, black arrow) when compared to Figures 2E and 3A. Interval increase in extent of focal nodular fat-stranding along transverse mesocolon, more extensive and measuring up to 4.7 cm in maximal thickness (Figure 4B, white arrow). Interval increased focal nodular fat-stranding in the right hypochondrium around hepatic flexure region, measuring up to 2.4 cm in thickness (Figure 4C, white arrows), when compared to Figure 3C.

TECHNIQUE: A total of 80ml of Omnipaque 350 was administered. Contrast-enhanced axial images in the soft tissue window, on portal venous phase.

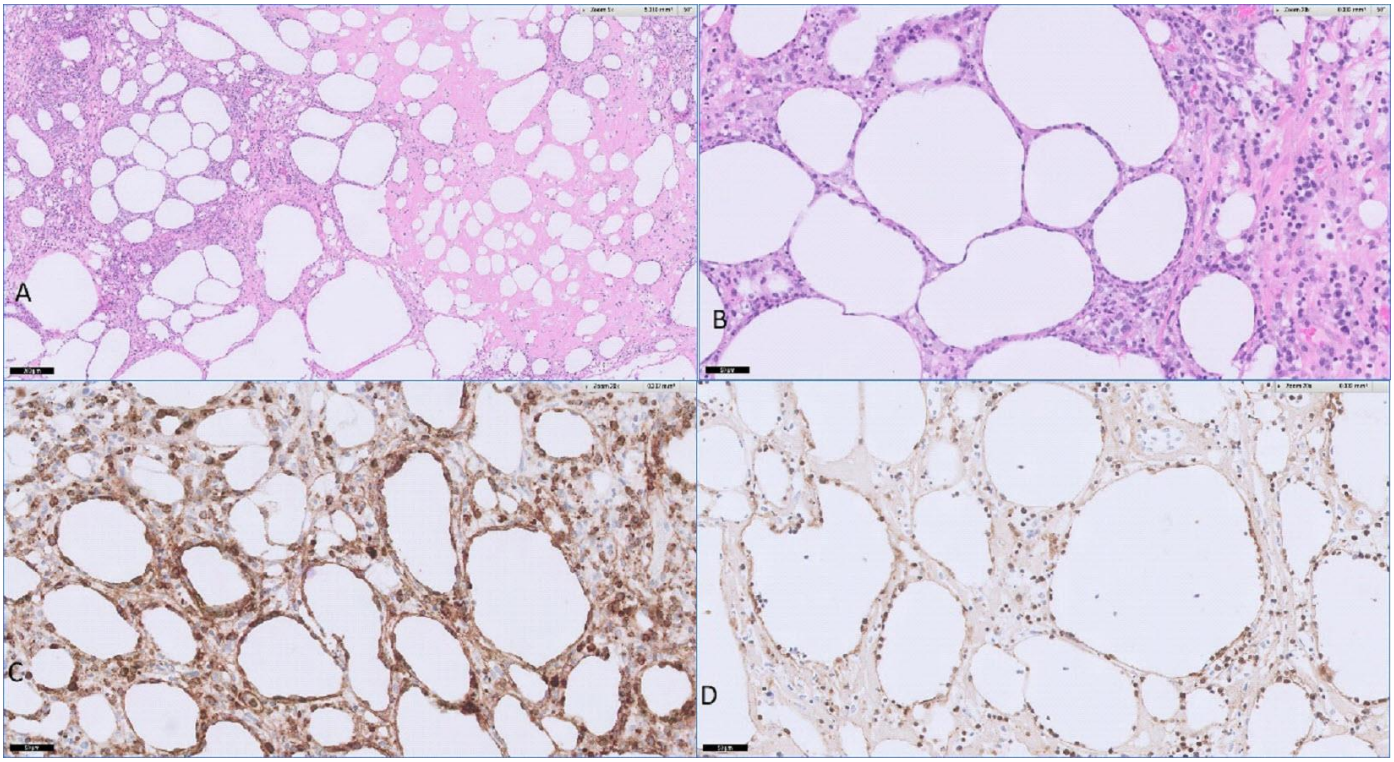

Figure 5: A 30-year-old gentleman with SPTCL where the primary disease is seen in the anterior abdominal omentum. Histology from the open biopsy of the anterior abdomen omentum is as described below:
Findings: H&E stain (magnification 5x) demonstrates panniculitis-like infiltrate of omental fat (Figure 5A). On higher magnification (20x), atypical lymphocytes are seen rimming adipocytes and in the interstitium (Figure 5B). The lymphomatous population retains its cytotoxic phenotype with positivity for Granzyme B (Figure 5C) as well as expression of T-cell hemireceptor (TChR)-beta F1 (Figure 5D). These findings are in keeping with involvement of refractory SPTCL.

Etiology	• Subclassification of skin lymphomas involving subcutaneous tissues; infiltration by neoplastic cytotoxic T-cells produces panniculitis-like pattern • Is now restricted to primary cutaneous lymphoma of the T-cell receptor αβ phenotype
Incidence	• Less than 1% of all non-Hodgkin's lymphoma
Gender ratio	• Female preponderance of 2:1
Age predilection	• Most common in young adults with median age of 36 years
Risk factors	• Unclear, not well-studied but possibly autoimmune
Treatment	• No current consensus on the gold standard of treatment but chemotherapy regime such as cyclophosphamide, hydroxydaunorubicin, Oncovin (vincristine), prednisolone and etoposide have been used with varying success on typical presentation of subcutaneous panniculitis-like T-cell lymphoma • No known treatment for atypical presentations
Prognosis	• Excellent in typical presentations with 5-year survival >80% • Unknown but likely much worse in atypical presentations
Imaging findings	• Ascites, splenomegaly and fat-stranding in the anterior abdomen on computed tomography • Areas of fat-stranding in the anterior abdominal omentum were avid on Fluorine-18 fluorodeoxyglucose positron-emission tomography

Table 1: Summary table of subcutaneous panniculitis-like T-cell lymphoma (with atypical presentation in the peritoneum).

Differential diagnoses	Imaging findings	Clinical findings
Subcutaneous panniculitis-like T-cell lymphoma presenting in peritoneum	• Ascites, splenomegaly and nonspecific fat-stranding in the peritoneum/anterior abdominal omentum on CT • Areas of fat-stranding on CT correspond to FDG-avidity on PET	• Fever, lymphadenopathy • Diagnosis confirmed on biopsy
Primary peritoneal serous carcinoma	• Ascites, peritoneal nodules/thickening and omental masses on CT with contrast enhancement • Psammomatous calcification sometimes seen in the nodules	• Almost always occurs in women • Abdominal distension and pain • Elevated serum Ca-125
Peritoneal malignant mesothelioma	• Presents as either diffuse involvement with sheet-like peritoneal thickening or focal intraperitoneal masses on CT • Ascites and omental caking also may be seen as fine nodular studding or masses • Omental masses demonstrate heterogenous enhancement	• Association with asbestos exposure • More common in men; median age 60
Peritoneal carcinomatosis	• Ascites with loculation may be seen • Findings on CT vary from multifocal discrete nodules to infiltrative masses • On CT, irregular thickening, nodularity and contrast enhancement of peritoneum • Infiltration of small bowel mesentery gives pleated or stellate appearance • MRI can be used for detecting subcentimetre nodules; also enhances on gadolinium • Will be FDG-avid on PET	• May initially be asymptomatic but can later present with abdominal distension and pain • Would have a known primary malignancy such as colorectal, ovarian, uterine, breast or lung
Tuberculous peritonitis	• Fibrotic type appears as large omental masses with nodular thickening with mesenteric caking and matting of bowel loops on CT • Dry type presents with mesenteric thickening, fibrous adhesions and caseous nodules. May have omental caking • Peritoneal thickening with contrast enhancement seen on CT	• Clinical features nonspecific • History of infection or exposure to tuberculosis may or may not be present
Sclerosing peritonitis	• Smooth thickening and enhancement of the peritoneum on CT • Peritoneal calcification may be seen but severe encapsulation can occur in the absence of it • Encapsulating peritoneal sclerosis gives appearance of "abdominal cocoon" • CT small bowel changes include mural fibrosis, thickening, adhesions and luminal narrowing	• Chronic fibrotic thickening of peritoneum encapsulating small bowel loops can eventually lead to recurrent small bowel obstruction • Aetiology unclear but has association with tuberculosis and sarcoidosis • Idiopathic form can affect both genders

Table 2: Differential diagnosis table for subcutaneous panniculitis-like T-cell lymphoma (with atypical presentation in the peritoneum).

ABBREVIATIONS

CHOPE = Cyclophosphamide, Hydroxydaunorubicin, Oncovin (Vincristine), Prednisolone and Etoposide
CT = Computed tomography
F-18 FDG = Fluorine-18 fluorodeoxyglucose
MR = Magnetic resonance
NHL = Non-Hodgkin's lymphoma
PET = Positron-emission tomography
SPTCL = Subcutaneous panniculitis-like T-cell lymphoma
SUV = Standardised uptake value
TCR = T-cell receptor
WHO = World Health Organisation

KEYWORDS

Subcutaneous panniculitis-like T-cell lymphoma; primary cutaneous lymphoma; peritoneum; anterior abdominal omentum; positron-emission tomography/computed tomography; PET/CT